

Research Paper

Identification of GPC3 mutation and upregulation in a multidrug resistant osteosarcoma and its spheroids as therapeutic target



Jun-Hua Nie^a, Tao Yang^b, Hong Li^c, Hai-Shan Ye^a, Guo-Qing Zhong^b, Ting-Ting Li^c, Chi Zhang^b, Wen-Han Huang^b, Jin Xiao^b, Zhi Li^d, Jian-Li He^c, Bo-Le Du^c, Yu Zhang^{b,*}, Jia Liu^{a,*}

^a School of Medicine, South China University of Technology, Guangzhou 510006, China

^b Department of Orthopedic Oncology, Guangdong Provincial People's Hospital Affiliated to South China University of Technology School of Medicine, Guangzhou 510030, China

^c Jingkeson BioMed Laboratory, Guangzhou Jingke Institute of Life Sciences, Guangzhou 510005, China

^d Department of Pathology, Guangdong Provincial People's Hospital Affiliated to South China University of Technology School of Medicine, Guangzhou 510030, China

ARTICLE INFO

Article history:

Received 24 June 2021

Revised 26 August 2021

Accepted 10 September 2021

Available online 20 September 2021

Keywords:

Osteosarcoma

Next generation sequencing

GPC3 mutation

Gene upregulation

Patient-derived spheroids

Multidrug resistance

Anti-GPC3 targeted therapy

ABSTRACT

Background: Drug resistance and the lack of molecular therapeutic target are the main challenges in the management of osteosarcomas (OSs). Identification of novel genetic alteration(s) related with OS recurrence and chemotherapeutic resistance would be of scientific and clinical significance.

Methods: To identify potential genetic alterations related with OS recurrence and chemotherapeutic resistance, the biopsies of a 20-year-old male osteosarcoma patient were collected at primary site (p-OS) and from its metastatic tumor (m-OS) formed after 5 months of adjuvant chemotherapy. Both OS specimens were subjected to cancer-targeted next generation sequencing (NGS) and their cell suspensions were cultured under three-dimensional condition to establish spheroid therapeutic model. Transcript-oriented Sanger sequencing for GPC3, the detected mutated gene, was performed on RNA samples of p-OS and m-OS tissues and spheroids. The effects of anti-GPC3 antibody and its combination with cisplatin on m-OS spheroids were elucidated.

Results: NGS revealed 4 mutations (GPC3, SOX10, MDM4 and MAPK8) and 6 amplifications (MDM2, CDK4, CCND3, RUNX2, GLI1 and FRS2) in p-OS, and 3 mutations (GPC3, SOX10 and EGF) and 10 amplifications (CDK4, CCND3, MDM2, RUNX2, GLI1, FRS2, CARD11, RAC1, SLC16A7 and PMS2) in m-OS. Among those alterations, the mutation abundance of GPC3 was the highest (56.49%) in p-OS and showed 1.54 times increase in m-OS. GPC3 transcript-oriented Sanger sequencing confirmed the mutation at 1046 in Exon 4, and immunohistochemical staining showed increased GPC3 production in m-OS tissues and its spheroids. EdU cell proliferation and Calcein/PI cell viability assays revealed that of the anti-OS first line drugs (doxorubicin, cisplatin, methotrexate, ifosfamide and carboplatin), 10 μ M carboplatin exerted the best inhibitory effects on the p-OS but not the m-OS spheroids. 2 μ g/mL anti-GPC3 antibody effectively committed m-OS spheroids to death by itself (76.43%) or in combination with cisplatin (92.93%). **Conclusion:** This study demonstrates increased abundance and up-regulated expression of mutant GPC3 in metastatic osteosarcoma and its spheroids with multidrug resistance. As GPC3-targeting therapy has been used to treat hepatocellular carcinomas and it is also effective to OS PDSs, GPC3 would be a novel prognostic parameter and therapeutic target of osteosarcomas.

© 2021 The Author(s). Published by Elsevier GmbH. This is an open access article under the CC BY-NC-ND license (<http://creativecommons.org/licenses/by-nc-nd/4.0/>).

Abbreviations: OS, osteosarcoma; PDS, patient-derived spheroids; p-OS, primary osteosarcoma; m-OS, metastatic osteosarcoma; NGS, next generation sequencing; MA, mutation abundance; NAC, neoadjuvant chemotherapy; FFPE, formalin-fixed, paraffin-embedded; H/E, hematoxylin and eosin; CDDP, cisplatin; CBP, carboplatin; DOX, doxorubicin; MTX, methotrexate; IHC, immunohistochemistry; MSS, microsatellite stable; SNV, single-nucleotide variant; GPC3-Ab, anti-GPC3 antibody.

* Corresponding authors.

E-mail addresses: luck_2001@126.com (Y. Zhang), mcliujia@scut.edu.cn (J. Liu).

<https://doi.org/10.1016/j.jbo.2021.100391>

2212-1374/© 2021 The Author(s). Published by Elsevier GmbH.

This is an open access article under the CC BY-NC-ND license (<http://creativecommons.org/licenses/by-nc-nd/4.0/>).

1. Introduction

Osteosarcoma (OS) is the commonest pediatric bone-derived malignancy with poor prognosis because of the early metastasis, difficulty of radical tumor removal and heterogeneity toward neoadjuvant chemotherapy [1]. According to International Childhood Cancer Classification (ICCCO), the 5-year survival rate of OS patients is the second lowest in childhood malignancies, for only 69%, and adolescent for 67% [2]. Only 20% of OS patients presents

with metastasis that is imaging detectable, while the majority of the remaining 80% bears undetectable micro-metastases at diagnosis [3,4]. Surgery is still the first choice in OS treatment, and neoadjuvant chemotherapy (NAC) is commonly used in order to shrink the tumor mass and to kill the spreading cancer cells for facilitating subsequent treatment [5]. Currently, NAC includes cisplatin, doxorubicin, high dose methotrexate and their combinations [6]. Although aggressive NAC has increased overall survival rate of localized OS cases, the poor survival rates for OS patients with metastasis or recurrence remains unimproved during the past decades [7] in term of less than 30% of post-relapse 5-year survival rate [8,9]. Because of the limited success of surgical resection and systemic chemotherapy for metastatic OS, it is necessary to explore new molecular target(s) to improve the therapeutic outcome of OS patients.

Large scale parallel next generation sequencing (NGS) is able to read DNA sequence, transcriptome and epigenome information from genome through sample preparation, cluster generation, sequencing and data analysis [10]. With this technology, hundreds of gene mutations have been found to be closely related to cancer formation, of which some determine drug sensitivity and, therefore, regarded as drug targets [11,12]. Currently, cancer-targeted NGS has been widely used to direct personalized therapy of colorectal [13], lung [14] and breast cancers [15,16]. In the case of osteosarcomas, some common gene mutations have also been detected by NGS but lack of the drug targetable ones as those found in other types of cancers [17]. Consequently, the clinical treatments of osteosarcoma remain almost unchanged during the decades [17]. It would be of scientific values and clinical significance to find out the novel genetic or epigenetic alteration(s) related to chemosensitivity and secondary drug resistance of osteosarcomas. In this context, cancer-targeted NGS performed on the paired primary and metastatic OS may help us to identify genetic alteration(s) related with tumor progression and drug resistance.

NGS test can reveal a large number of genetic information, while the proportion of genetic alterations that can be used to guide drug use is still limited at current stage [18]. For instance, only 0.4% of tumor-related genetic variants has corresponding FDA approved targeted drugs and another 9.6% of gene variants might become potential therapeutic targets [18]. The situation of OSs is even dim as none of the current targetable mutations has been so far detected in them [19]. Moreover, the heterogeneity of cell composition in OSs leads to even poor chemotherapeutic consequence. Therefore, there is an urgent need for a new drug sensitivity detection system that can select the drugs suitable for individual OS case from the existing anti-OS agents.

Patient-derived spheroids/PDSs are cell spheroids formed by cancer cell suspension under 3D culture condition. As PDSs largely retain the biological characteristics of their original tumor, they are very suitable for validation of NGS-generated genomic data, the analyses of high-throughput drug screening and detection of the factors related with drug response [20]. This platform is particularly valuable for OSs that lack of targeted drugs and rely on chemotherapeutic strategy. For this reason, a pair of primary and metastatic tumors was collected from a 20-year-old OS patient, which were undergone cancer-targeted NGS and spheroid-based drug sensitivity assay, so as to find potential genetic markers closely related to drug sensitivity and prognosis of OSs.

2. Materials and methods

2.1. Ethical approval and consent to participate

The contents of this study were reviewed and approved by the Research Ethics Committee of Guangdong Provincial People's Hospital, Guangdong Academy of Medical Sciences (No.

GDREC2020093A). The samples used in current study were collected from the Department of Orthopaedic Oncology, Guangdong People's Hospital, Guangzhou, China, and the written informed consents were obtained from the patients and/or his immediate relative (s) with recognized guidelines. This research project was conducted according to the guidelines and approval of biomedical ethics.

2.2. Surgical specimens and pathological classification

The fresh specimens of a 20-year-old male OS patients were collected from the primary growth site by bone puncture biopsy and from the metastatic tumor at the time of operation 5 months after neoadjuvant chemotherapy. The tissues obtained were separated to several parts for three dimensional spheroid culture, the frozen tissue section and DNA isolation, respectively. The remaining specimens were formalin-fixed, paraffin- embedded and sectioned for hematoxylin and eosin (H/E) staining. The stained slides were evaluated by the experienced orthopedic pathologists to confirm the diagnosis.

2.3. Sample preparation for NGS sequencing

The surgical samples were received freshly within 2 h, which were placed in transport medium containing advanced DMEM/F12 (Gibco, 12634010), 100 U/mL penicillin (Gibco, 10378016), 100 µg/mL streptomycin (Gibco, 10378016) and 20 µg/mL nystatin (Sangon Biotech, 89104730). The representative part of them was incised to prepare cell suspension for spheroid production. The remaining sample was snap-frozen for frozen section and DNA extraction. Genomic DNA was extracted from tumor tissue and paired blood samples with the DNAeasy Blood and Tissue kit (Qiagen, 69504) according to the manufacturer's instructions. DNA sample was quantified using the Nanodrop 2000c (Thermo Fisher, USA) and the Qubit High Sensitivity dsDNA assay (Thermo Fisher, Q32851).

2.4. Library preparation, sequencing and data analysis

A total of 550 genes that are closely related with cancer formation and progression were selected for capture. Genomic DNA was sheared via sonication while using an S220 focused-ultrasonicator (Covaris, 500217, USA) to produce fragmented genomic DNA (500 ng) and DNA libraries were constructed using the KAPA Hyper Prep kit (KAPA) following the "with beads" manufacturer protocol. DNA libraries were analyzed on TapeStation to verify correct fragment size and to ensure the absence of extra bands. Samples were quantified using KAPA qPCR quantification kit. The captured libraries were sequenced using the Illumina HiSeq X platform with paired-end sequencing runs (2 × 150) under Illumina recommended protocols. Raw reads were checked and filtered with Fastp with default parameters [21]. The filter reads were aligned to the human reference genome hg19 with the BWA-MEM algorithm [22]. Optical and PCR duplicate were marked using picard and local realignment around indel region was performed using GATK [23]. For cases with matched normal samples, the somatic mutations were identified using MuTect2 with default settings [24]. Copy number aberrations were identified by cnvkit and manually annotated as reference [25,26]. High quality variants were further filtered by 1000 Genomes (20110521 release), ESP6500, ExAC, and CG46 (popfreq_max_20150413), provided by ANNOVAR to remove the potential SNP sites [27]. Annotation of variants were carried out with ANNOVAR [27].

2.5. Spheroid culture

This experiment was conducted according to the protocol for generating human osteosarcoma spheroids [28,29]. After three

washes in PBS, the tumor samples were minced into small particles (less than 0.1 mm diameter) on ice. The minced tissues were incubated with 1 mL TrypLE (Gibco, A1217701) for 45 min at 37 °C and washed with DMEM (Gibco, 14190250) containing 500U penicillin, 500 µg/mL streptomycin and 50 µg/mL nystatin. After digestion, the cell suspension was filtered through a 70-µm cell strainer to remove undigested large fragments and centrifuged at an average of 300 rpm for 5 min to pellet cells. The isolated cells were re-suspended in a complete culture media and mixed with a 1:2 vol of Matrigel matrix (Corning, phenol red free, 356237). 3D culture was performed in the form of about 5000 cells/30µL droplet/well (48-well plate). After allowing the Matrigel polymerize, complete medium was added and the cell left at 37 °C and was changed by in two-day intervals. The complete medium contains DMEM/F12 with L-Glutamine and Sodium Bicarbonate (Gibco, 12634010), 10% fetal bovine serum (FBS, Australia, Gibco, 10099141), 100 U/mL Penicillin, 100 µg/mL Streptomycin (Gibco, 15070063), Nystatin 20 µg/mL (Sangon Biotech, 89104730), Nicotinamide 10 mM (Sigma, N0636), N-Acetylcysteine 1 mM (Sigma, 106425), A83-01 0.5 µM (Tocris, 909910), B-27 minus vitamin A 1x (Invitrogen, 12587010), EGF 50 ng/mL (Peprotech, AF-100-15), RSPO1 500 ng/mL (Peprotech, 120-38), SB-202190 10 µM (Sigma, 152121), 10 µmol/L Rock inhibitor Y-27632 (Sigma-Aldrich, HY-10071) and 0.01 ng/mL Noggin (Medical Chemical Express, HY-P7086). The proliferating OS tumoroids were serially passaged every 3 weeks by dissociation with 250-500µL TrypLE Express (Gibco, A1217701). The spheroids of this OS case keep alive over 3 months before frozen storage for future use.

2.6. OS-spheroid-based drug sensitivity assays

Drug sensitivity assays were conducted on primary and metastatic OS spheroids by the use of 1 µM doxorubicin/DOX (Med-CheExpress, MCE, HY-15142) [30], 4 µM cisplatin/CDDP (MCE, HY17394) [31], 10 µM methotrexate/MTX (MCE, HY-14519) [30], 10 µg/mL (MCE, HY-17419) ifosfamide/IFO [32] and 10 µM carboplatin/CBP (MCE, HY-17393) [33]. The treatments lasted for 96 h. The second-line drugs including 10 µM palbociclib/PAL (MCE, HY-50767) [34], 20 µM etoposide/EPEG (MCE, HY-13629) [35] and 1 µM vinorelbine/NVB (MCE, HY-12053) [36] were employed to treat the metastatic OS spheroids. After 72-hour drug treatments, the spheroids were incubated overnight in a medium containing 10 µM EdU (Beyotime Biotech. Inc. Shanghai, China; C0078L) permeable red fluorescent dye for cell proliferation test. TUNEL cell apoptosis detection kit (Beyotime, C1088) was used to detect the apoptotic cells in the spheroids by the methods described elsewhere [37]. In parallel, cell viability and death of the experimental groups were elucidated using a Calcein/PI cell viability detection kit (Beyotime Biotech. Inc. China, C2015) and trypan blue viable/nonviable cell discrimination assay. Briefly, the spheroids were incubated in cell recovery solution (CRS) under 4 °C for 30 min by the end of drug treatments. When spheroids were disassociated completely in CRS, they were washed and enrich in PBS. The spheroids were incubated with trypan blue or calcein/PI dye solution. Trypan blue-stained dead and -unstained living cells in the individual spheroids were counted under phase contrast microscope (Nikon, Eclipse Ts2). The dead cells with PI-labeled red nuclei and the viable cells with calcein-labeled green nuclei were counted under the fluorescent microscope (Carl Zeiss, Axio Imager2). Over 50 spheroids in each of the experimental groups were counted. The experiments were repeated for three times to get the reliable results.

2.7. Immunohistochemical staining

By the end of experiments, the spheroids were harvested and fixed in 4% paraformaldehyde for 60 min. The fixed spheroids

were re-suspended in 2% warm agarose. OTC-embedded fixed spheroid and tissues were sliced into 5 µm sections. The frozen tissue sections were fixed by cold acetone for 20 min. Spheroid and tissue slices were conducted to Hematoxylin and Eosin Staining Kit (Leagene, 082A20). In parallel, immunohistochemical staining was performed by the method described elsewhere [38]. The rabbit anti-human GPC3 antibody (Abcam, ab174851) were used in the dilution rates of 1:500. Color reaction was developed by DAB Horseradish Peroxidase Color Development Kit (Beyotime, P0203).

2.8. CD133 and GPC3 double immunofluorescent labeling

CD133 and GPC3 double immunofluorescence labeling was performed on tumor tissue and spheroids. The tumor tissues and spheroids were rinsed with PBS, and then fixed by 4% paraformaldehyde for 60 min. After blocked with 10% goat serum in PBS for 20 min, samples were incubated overnight at 4 °C with rabbit anti-CD133 antibody (1:200; Bioss, 5814R) and mouse anti-GPC3 (1:500; Cell Marque, 261 M-94). Followed by co-incubation with Coralite488-conjugated goat anti-rabbit IgG and Coralite594-conjugated goat anti-mouse IgG (both in 1:500; Peprotech) at 37 °C for 1 h. Nuclei were labeled with Hoechst 33,342 and captured by fluorescence microscope (Nikon, ECLIPSE Ni-U).

2.9. Detection of mutant GPC3 transcripts via Sanger sequencing

The high quality mRNA of fresh tissue was sliced by freezing microtome and the slices were kept in RNA ladder. The tissues were harvested for RNA extraction with the RNAeasy animal RNA isolation kit with spin column (Beyotime, Shanghai, China). As for spheroids, RNA was extracted by single cell/low input RNA library prep kit for illumina (NEBNext, Hertfordshire, UK, E7530L). After that, the RNA concentrations were measured by Nanodrop 8000 (Thermo, USA). In order to detect the RNA completeness without DNA contamination, we use RNA gel electrophoresis. After that, extracted RNA was reverse transcribed into first strand cDNA using PrimeScript RT reagent kit (Takara, RR037B). And real-time PCR were performed in triplicates using PremixTaq (Takara, R004A) and Applied Biosystems Veriti 96-well Thermal Cycler (Thermal, USA). The amplified DNA were also quantified by Qubit High Sensitivity dsDNA assay. Housekeeping gene β-actin was used for normalization. Gene specific primers for GPC3 and β-actin were designed by Primer Express (Sangon Biotech, Shanghai, China). The primer sequences are GPC3 5' to 3'- GTCCTTGAAGAAGACTTGT [39] and 3' to 5'- TAGTTCCTTCTTCGGCTG (designed by Accurate Biology); β-actin 5' to 3'- CTCCATCTGGCCTCGCTGT and 3' to 5'- GCTGTACCTT-CACCGTTC [40]. 2 µL of 271 bp GPC3 PCR products from individual experimental groups were undergone electrophoresis and the remaining parts were subjected to Sanger sequencing. β-actin was cited as internal qualitative and quantitative control.

2.10. Spheroid treatment with anti-GPC3 antibody

The anti-Glypican-3/GPC3 mouse monoclonal antibody was purchased from Cell Marque (California, USA, 261 M-94) for the use of GPC3-targeted therapy. The spheroids generated from the primary and metastatic tumors were treated by gradient concentrations (0.5, 1, 1.5 and 2 µg/mL) of the antibody for 96 h. By the end of the treatments, the spheroids were checked by EdU proliferation assay, TUNEL apoptosis assay with the methods described elsewhere [37]. Trypan blue viable/nonviable cell discrimination assay and Calcein/PI cell viability assay were employed to determine cell death rates of the experimental groups by the procedures

described above. The experiments were repeated for three times to establish confidential conclusion.

3. Results

3.1. Osteosarcoma and its post-chemotherapy metastasis

The 20-years old male patient without family cancer history was diagnosed with osteosarcoma in Guangdong Provincial

People's Hospital. Enhanced CT revealed a 15.7 cm × 11.8 cm tumor mass with a smooth surface arising on the left humerus, multiple round low-density shadows are seen inside. The tumor parenchyma is unevenly strengthened, with local bone destruction on the left scapula, and the surrounding soft tissues is swell (Fig. 1A and 1B). The tumor was surgically removed shortly after diagnosis. Pathological examination revealed scattered osteoclast-like multinucleated giant cells with obvious atypia, spindle-like phenotype and increased nuclear fraction (Fig. 1C).

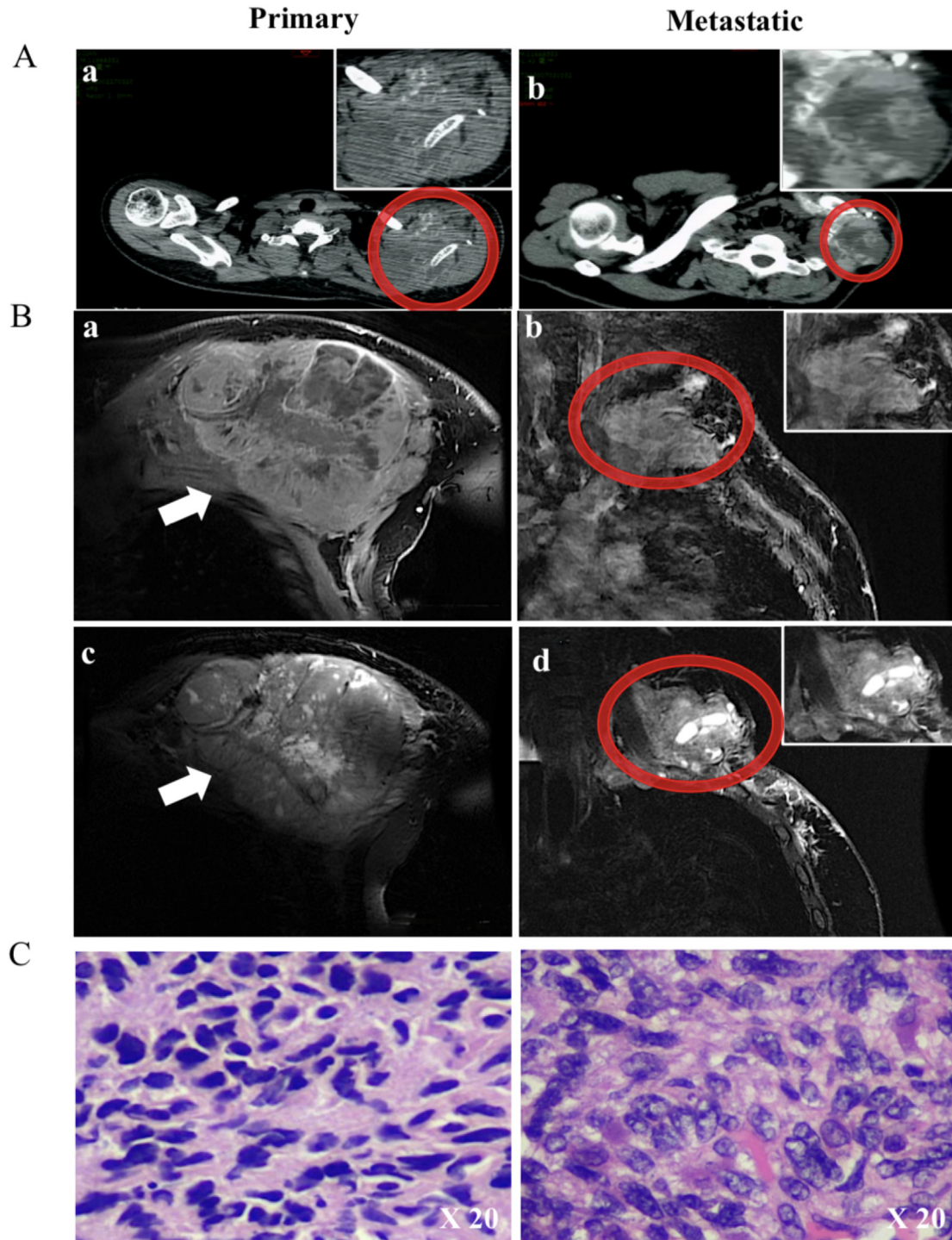


Fig. 1. CT, MRI and morphological images of primary osteosarcoma and its metastasis. (A) CT image of the shoulder in a 20-year-old man with left humerus osteosarcoma. (a) On primary, CT showed a large, well-defined irregular mass at humerus. (b) On metastasis, CT showed an invasive mass on left neck and shoulder. (B) Coronal sections MRI image of the shoulder on primary and metastasis OS as upper. (a), (b) belongs to T1 + contrast, (c), (d) are T2 weighted images. (C) HE morphological staining of the primary and metastatic tumors.

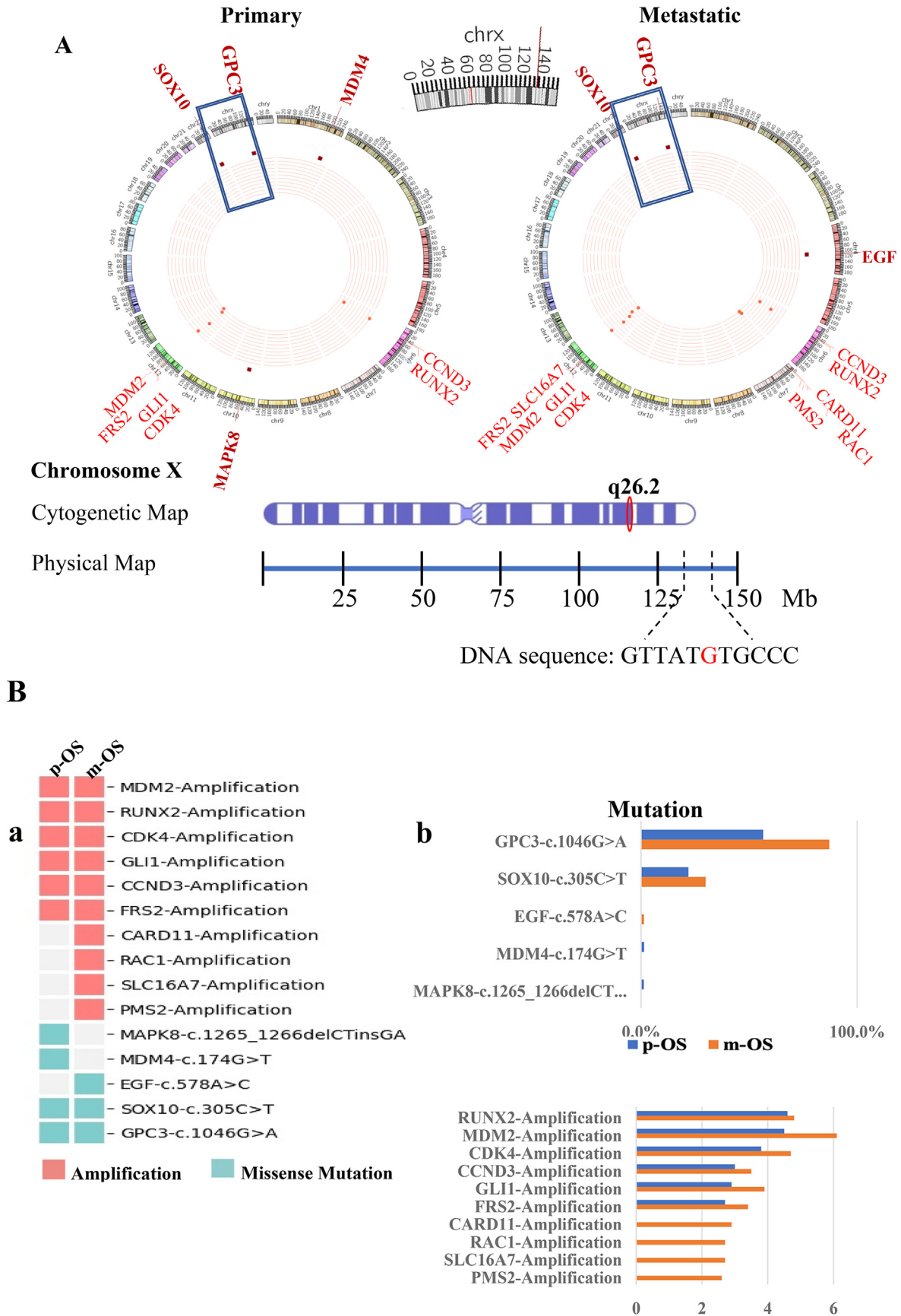


Fig. 2. NGS detection of GPC3 mutation in the primary and metastatic osteosarcomas. (A) Representative Circos plots of the different molecular subtypes of primary osteosarcoma and its metastatic counterpart; Cytogenetic map of chromosome X and physical map of GPC3 mutation. **(B)** Gene mutation sites and mutation abundance of the primary and metastatic osteosarcomas. (a) mutation sites; (b) mutation abundance.

Five months after neoadjuvant chemotherapy, CT and MRI showed the absence of tumor formation at original site (left upper extremity) but a new tumor mass was observed between left shoulder and neck, and the high-density shadow of left subclavian vein to the superior vena cava indicated the tumor thrombus formation (Fig. 1A and 1B). Left scapula and neck mass resection was conducted and the postoperative pathological examination diagnosed the removed tumor again as osteoblastic osteosarcoma (Fig. 1C). The adjuvant chemotherapy was conducted using high-dose methotrexate (MTX), cisplatin (CDDP), doxorubicin (DOX) and ifosfamide (IFO) but failed to suppress tumor growth.

3.2. Altered somatic mutation spectrum of primary and metastatic OSs

In order to identify somatic mutations, cancer-targeted NGS covering 550 cancer-related genes was performed on the DNA samples prepared from the primary and metastatic OS tissues, respectively [41]. The results revealed 10 somatic alterations (GPC3, SOX10, MDM4, MAPK8 mutations and MDM2, CDK4, CCND3, RUNX2, GLI1, FRS2 amplifications) in primary tumor tissue and 13 somatic alterations (GPC3, SOX10, EGF mutations and CDK4, CCND3, MDM2, RUNX2, GLI1, FRS2 CARD11, RAC1, SLC16A7, PMS2 amplifications) in its metastatic counterpart, of which 3 (CDK4, CCND3 and MDM2) had clear or potential clinical significance (Fig. 2A and 2B). The cancer tissues are microsatellite stable (MSS) with 4 single-nucleotide variants (SNVs) in primary cancer tissue and 3 SNVs in the metastatic one.

3.3. Increased GPC3 mutation abundance in metastatic tumors

To demonstrate the heterogeneity of this OS case, the mutation profiles of primary and metastatic tumor specimens were analyzed and then mutation clonal clustering were performed to aggregated 9 sub-clones (Fig. 3). For these 9 clones, we plotted the clonal evolution and generated the phylogenetic tree. It was found that the mutated clone with GPC3 take the majority (Fig. 3). GPC3 is a member of heparan sulfate proteoglycans, which attaches to the cell membrane and is frequently expressed in hepatocellular carcinomas (HCCs) as an therapeutic target. The GPC3 mutation rate is 56.49% in the primary tumor and raised to 87.06% in the metastatic one, indicating that the tumor cells harboring mutant GPC3 became predominant in the metastatic cells (Fig. 3).

3.4. Mutant GPC3 upregulation in metastatic tumor and spheroids

To clarified whether GPC3 gene is expressed after mutation, GPC3-oriented RT-PCR and quantitative RT-PCR/qPCR were per-

formed on the RNA samples of primary and metastatic tumors. RT-PCR generated 271 bp GPC3 product in primary tumor and its spheroids, which showed 2.04 time increase in the metastatic tumor and 1.67 time increase in the metastatic tumor-derived spheroids (Fig. 4A); qPCR showed 2.78 time increase of GPC3 expression in the metastatic tumor and 2.92 time increase in metastatic tumor-derived spheroids in comparison with that of their primary counterparts (Fig. 4B). The following Sanger sequencing demonstrated that the GPC3 transcripts with 'G' to 'A' point mutation at the position of 1046 in Exon 4 were detected in the primary tumors and spheroids, which became abundant in the metastatic tumor and spheroids (Fig. 4C).

3.5. Increased GPC3 production in metastatic OS cells

The histological, the biological and differentiation features of the primary and metastatic OSs are well maintained by their spheroids in terms of the similar phenotype, SOX9/Vimentin co-expression [42,43] and CD133 production (Fig. 5A-D). The spheroids were formed within 10 days and kept growth after serial passages until frozen storage (Fig. 5B). Double immunofluorescent staining revealed that the OS specific marker SOX9 (green-labeled) is labeled in the nuclei and vimentin (red-labeled) is labeled on the membrane of primary and metastatic OS tumors and their spheroids (Fig. 5C). Immunofluorescent staining also showed that GPC3 was detectable in the cytoplasm and membrane of primary OS tumor and spheroids, and became intensified in their metastatic counterparts (Fig. 5D). At the same time, the green-labeled CD133 and the red-labeled GPC3 were detected in the primary and became strong positive in the metastatic OS tissue and spheroids (Fig. 5D).

3.6. Distinct response of p-PDS and m-PDS to chemotherapy

Tumor spheroids derived from the primary (p-PDS) and metastatic osteosarcoma specimens (m-PDS) were subjected to drug sensitivity test, using 4 first line anti-osteosarcoma drugs (doxorubicin/DOX, cisplatin/CDDP, methotrexate/M, ifosfamide/I) and carboplatin/CBP. The results revealed that those drugs exerted inhibitory effects on the primary osteosarcoma spheroids, of which CBP caused 94.36%, ifosfamide caused 86.15%, CDDP caused 79.79%, doxorubicin caused 75.1% and methotrexate caused 53.73% of cell death after eliminating natural mortality (Fig. 6A and 6C). The response of metastatic spheroids to those drugs became poor in terms of 55.14% of cell death in doxorubicin-treated, 41.5% in ifosfamide-treated, 39.26% in CBP-treated, 32.13% in methotrexate-treated group and 20.45% in CDDP-treated group when natural cell death were eliminated (Fig. 6B and 6C).

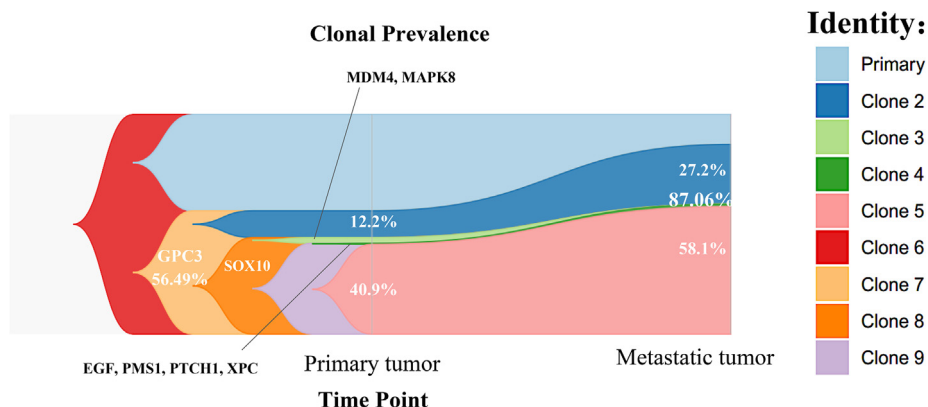


Fig. 3. Schematic diagram of osteosarcoma patient's evolution tree. GPC3 mutation abundance was 56.49% in the primary tumor and 87.06% in the metastatic one, indicating that the mutant GPC3 harboring OS cells became predominant as tumor progression.

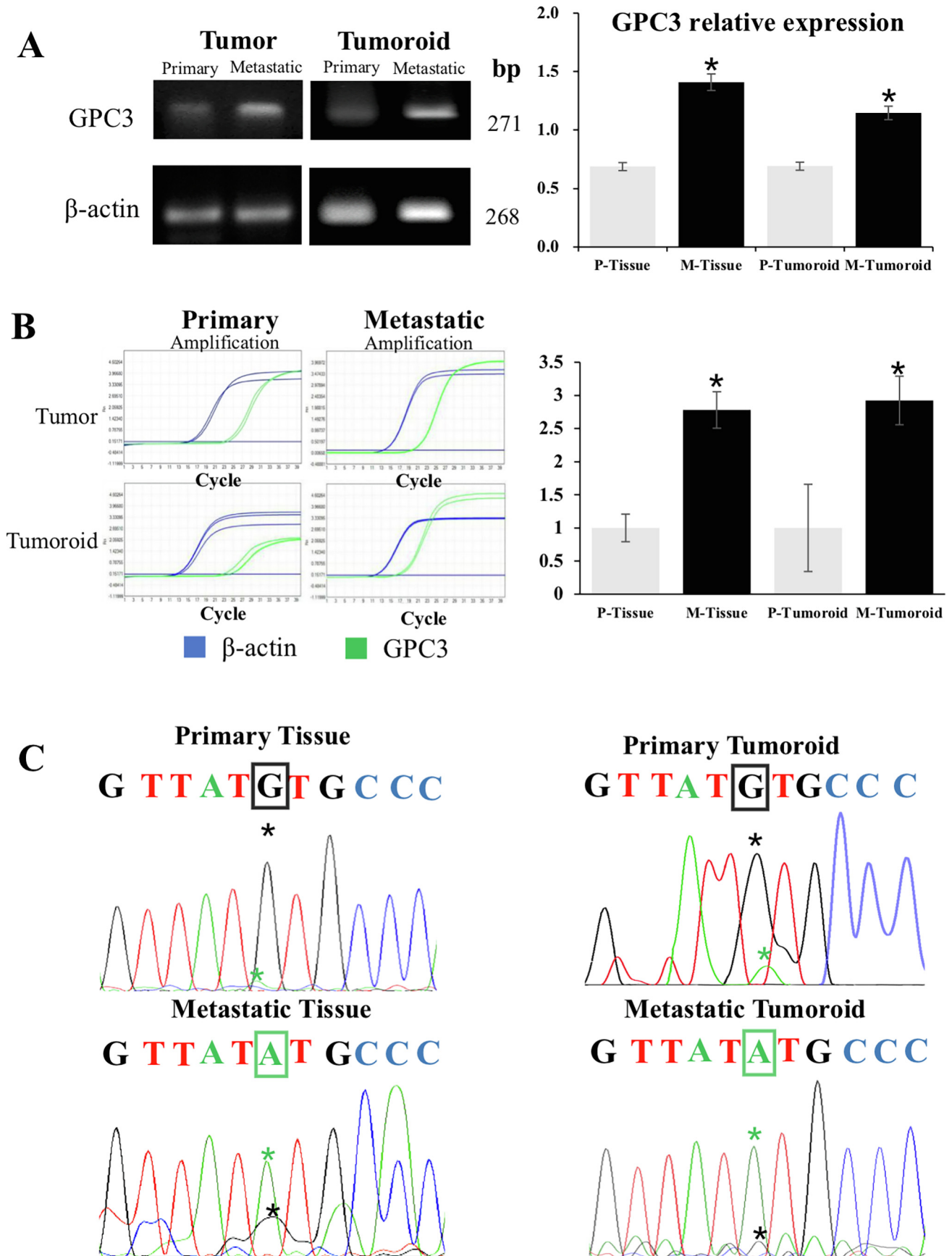


Fig. 4. Increased abundance of GPC3 mutation in the metastatic osteosarcoma. (A) Reverse transcription polymerase chain reaction detected GPC3 expression and Gray value analysis of GPC3 expression between the primary and metastatic OS tissue and their spheroids. (B) qPCR quantification of GPC3 expression in primary and metastatic OS tissues and spheroids. (C) Sanger sequencing analysis of GPC3 transcripts demonstrated G to A mutation in Exon 4.

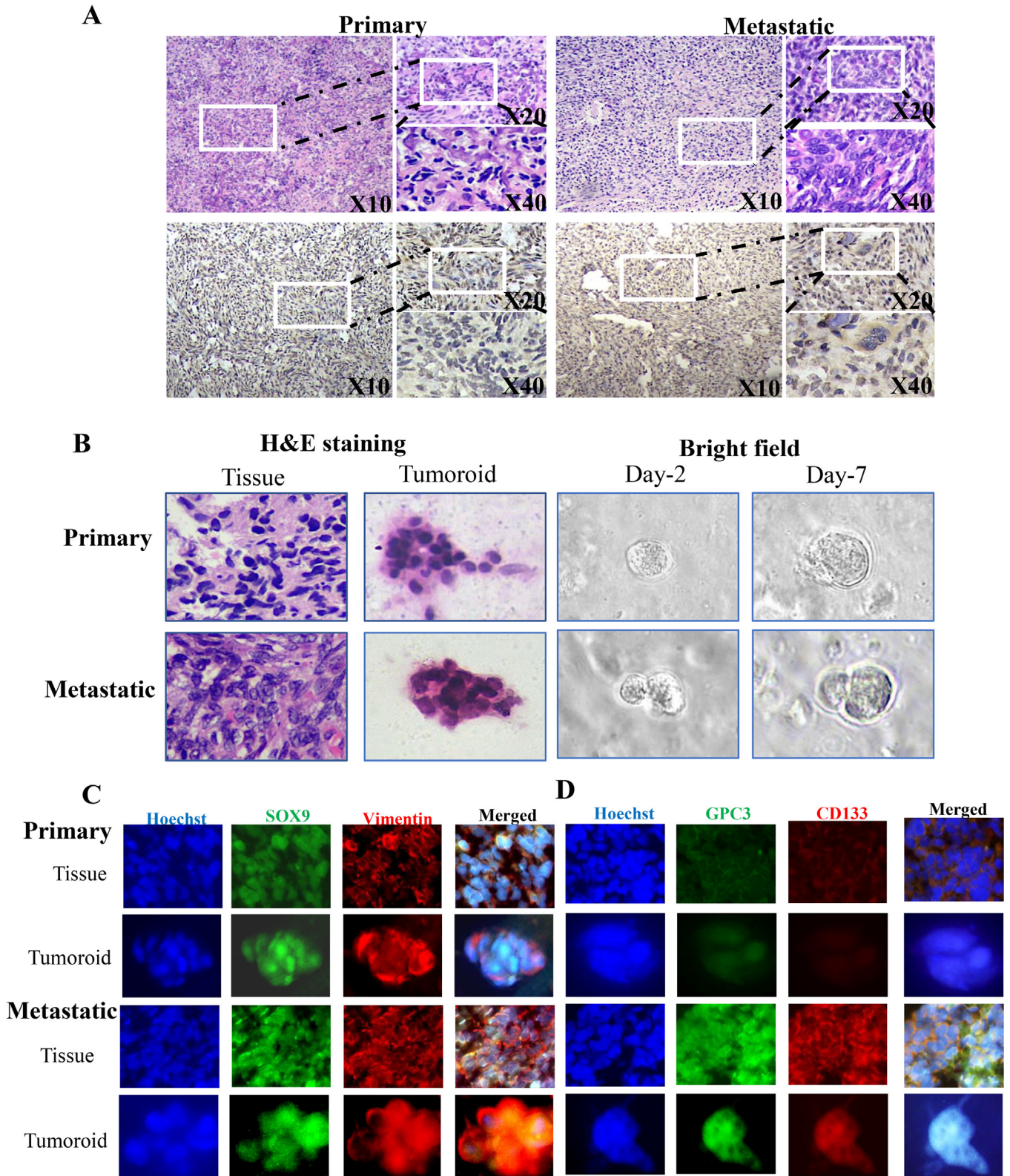


Fig. 5. Morphology and GPC3 expression of primary and metastatic osteosarcoma tissues and their spheroids. (A) H&E staining of primary and metastatic OS tissue under different magnification. **(B)** Bright field and HE demonstration of primary and metastatic OS tissues and their spheroids (X 20). **(C)** SOX9 (green) and vimentin (red); **(D)** GPC3 (green) and CD133 (red) immunofluorescence imaging of the primary and metastatic tumors and their spheroids (X10). (For interpretation of the references to color in this figure legend, the reader is referred to the web version of this article.)

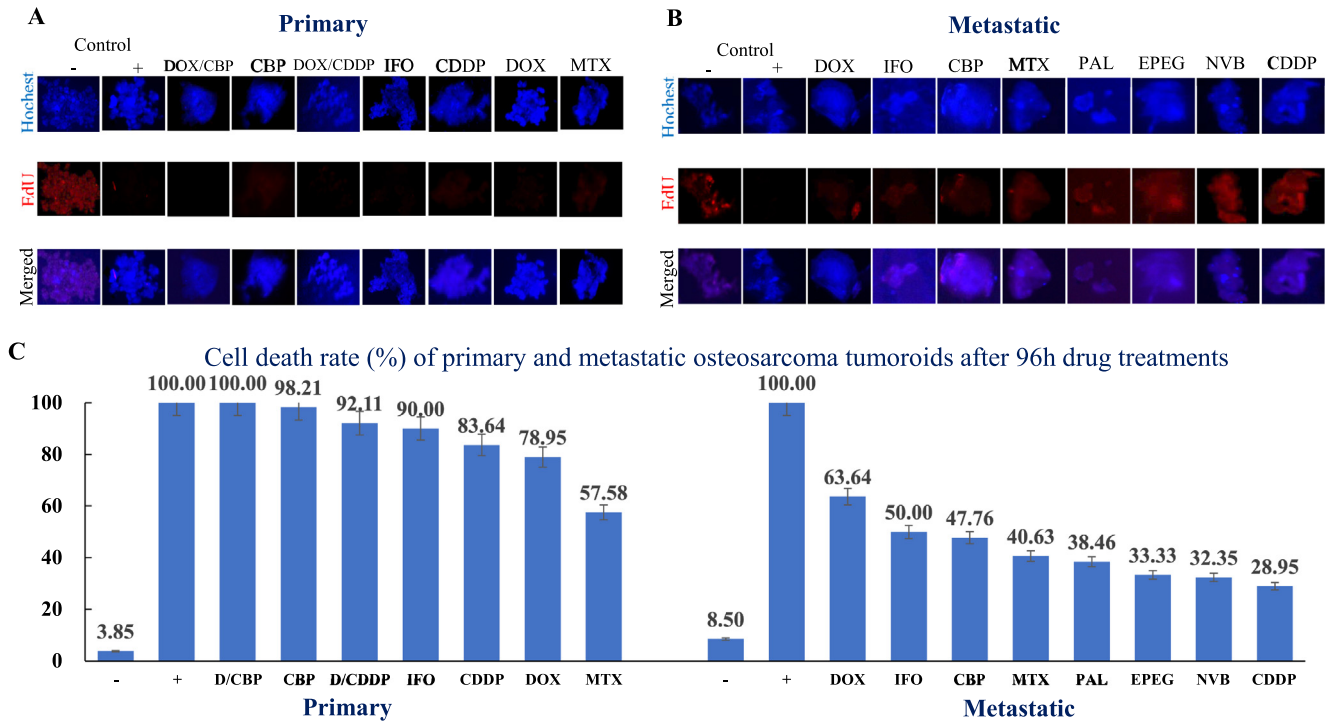


Fig. 6. Drug response of patient-derived OS spheroids of the primary and metastatic tumors. EdU proliferation and Calcein/PI cell viability assays performed on the primary (A, C) and the metastatic spheroids (B, D) after 96 h drug treatments. (-: negative control; +: positive control; DOX: doxorubicin; CBP: carboplatin; CDDP: cisplatin; IFO: ifosfamide; MTX: methotrexate; PAL: palbociclib; EPEG: etoposide; NVB: vinorelbine.)

3.7. Suppression of PDSs by GPC3-targeted therapy

The targeted-therapy with anti-GPC3 antibody (GPC3-Ab) has been used in multiple cancer clinical trial [44]. GPC3-positive metastatic OS spheroids (m-OS spheroids) were treated by GPC3-Ab in the doses of 0, 0.5, 1 and 2 μg/mL respectively and then by 1 μg/mL GPC3-Ab and 4 μM cisplatin combination. EdU cell proliferation test and TUNEL assay showed that GPC3-Ab caused growth suppression and apoptosis of m-OS spheroids in dose-related fashion (Fig. 7A). The results of Calcein-PI cell viability assay were consistent with the above findings (Fig. 7B 7C). The m-OS spheroids were resistant to 4 μM cisplatin but 92.93% of their cells died of apoptosis after 96 h of 1 μg/mL GPC3-Ab/4 μM cisplatin treatment (Fig. 7C).

4. Discussion

Osteosarcoma (OS) is the most common primary bone malignancy, of which 53% occurs among children and adolescents [46]. It therefore seriously affects the physical and mental health, life quality and even life of this young group [47]. Surgery is the main treatment for osteosarcoma, while the survival rate of osteosarcoma patients with surgery alone is only 15% – 17% [48]. The application of high-dose methotrexate, doxorubicin, cisplatin and ifosfamide as neoadjuvant chemotherapy (NAC) increased the patients' survival rate by 3 times [49], but the patients suffered from a series of adverse reactions during and after treatment. Moreover, some OS patients bear small metastases at the time of diagnosis, whose prognosis is even worse [50]. This situation is also hold true in the case reported here. The 20-year-old male patient was diagnosed with osteosarcoma of the left upper limb. 5 months after neoadjuvant chemotherapy and surgery, the second tumor appeared at shoulder and neck. Pathological examination confirmed that the primary and secondary tumor shared similar

histopathological phenotype of osteosarcoma. Because conventional anticancer drugs had been used in NAC and postoperative chemotherapy, the recurrent tumor would process the capacity of multidrug resistance. Therefore, it is necessary to analyze the genomic features of the recurrent or metastatic tumors and compare with that of its primary counterpart. To explore the internal mechanism leading to drug resistance and to find potential target (s) for the treatment of osteosarcoma, the patient-derived spheroids would be required to conduct drug sensitivity assay and to evaluate the difference of chemo-sensitivity between the primary and metastatic tumors.

Cancer-targeted NGS (Ct-NGS) sequencing is able to discover genetic alterations closely related to cancer formation and progression, and to provide evidence and important clues for individualized anticancer therapy [51]. Therefore, Ct-NGS covering 550 cancer-related genes was performed on the primary and recurrent tumor tissues as the first experimental step [41]. The results revealed 10 somatic mutations and 6 germline mutations in primary tumors, including GPC3, SOX10, MDM4 and MAPK8 missense mutations. In the case of the metastatic tumor, only an additional EGF missense mutation with the mutation abundance of 1.33% was detected. It should be noted that the mutation abundances of GPC3 and SOX10 were the highest in primary one, and the former increased from 56.49% to 87.06% (1.54 times) and the latter increased from 21.9% to 29.86% (1.36 times) in the recurrent tumors, while MDM4 and MAPK8 became no more detectable in the metastatic tumor. The above evidence suggests that the distinct increase of GPC3 mutation abundance in the metastatic OS cells is a nonrandom event with certain biological significance.

Currently, the association of SOX10 [52], MDM4 [53], MAPK8 [54], MDM2 [55], CDK4 [56], CCND3 [57], Runx2 [58], Gli1 [59], FRS2 mutation [55] with osteosarcoma formation has been documented, while no report is so far available concerning GPC3 muta-

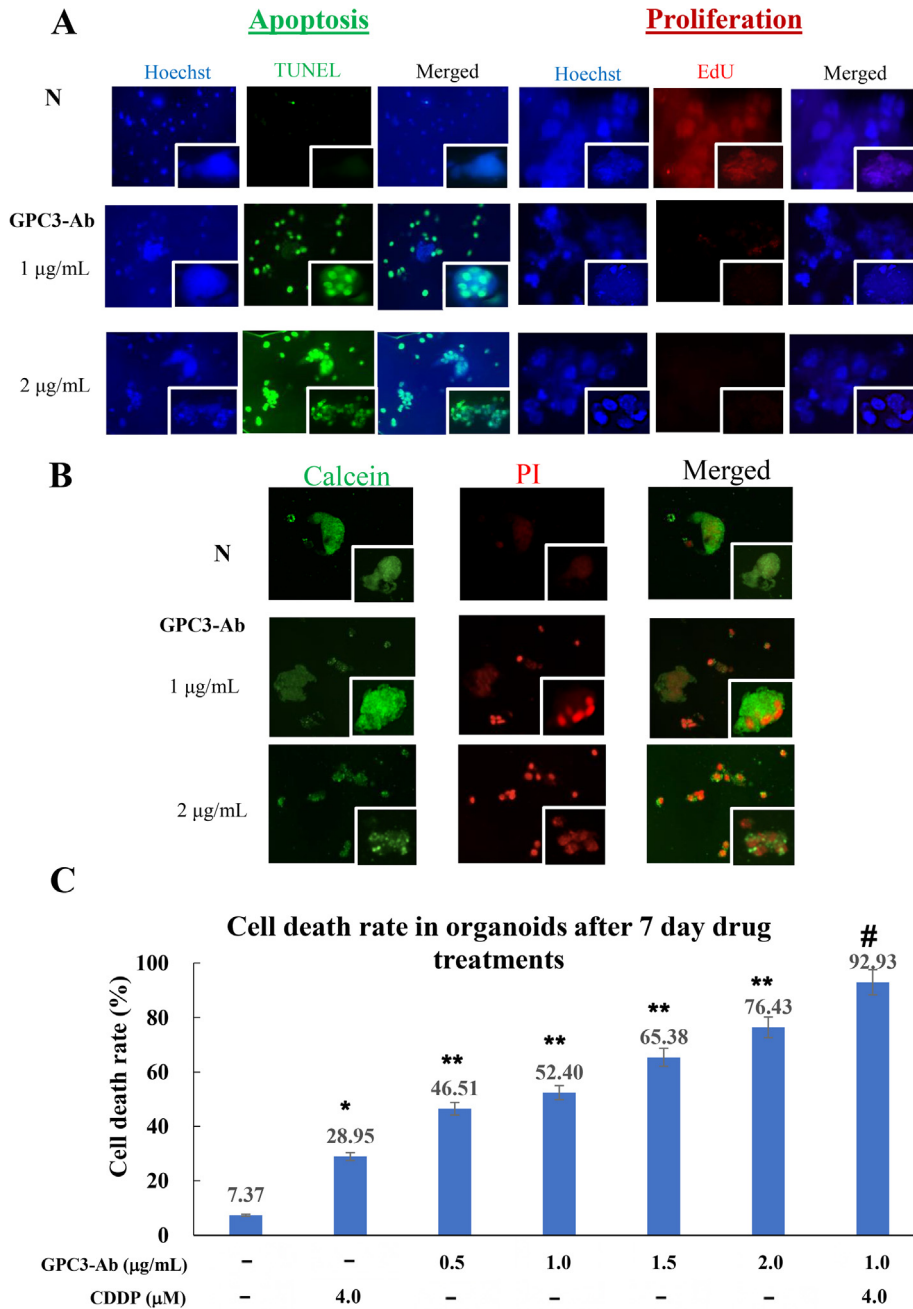


Fig. 7. GPC3 targeted therapy performed on metastatic OS spheroids. (A) Apoptosis and proliferation of m-OS spheroids labeled by TUNEL and EdU under anti-GPC3-antibody (GPC3-Ab) treatment. (B) Cell death rate of m-OS spheroids treated by gradient GPC3-Ab, 4 µM cisplatin, and GPC3-Ab/cisplatin, combination. *, $p = 0.013$ in comparison with normal culture group; **, $p = 0.00046, 0.00049, 0.00026$, in comparison with normal culture group; #, $p = 8.44 \times 10^{-5}$ in comparison with 2.0 µg/mL GPC3-Ab treated group.

tion and expression in osteosarcomas especially those with metastasis and/or multidrug resistance. It has been found that GPC3 is an oncofetal protein expressed in 72% of hepatocellular carcinomas [60] and 97% in hepatoblastomas [59]. Because GPC3 is absent in normal liver tissues as well as the benign liver diseases such as liver cirrhosis and fatty liver, it has been regarded as a target for targeted-therapy of hepatocellular carcinoma [60], and GPC3-targeting therapy has been proved effective in clinical practice [61]. Additionally, high frequency of GPC3 expression was also found in Wilms tumor (58%), malignant rhabdomyosarcoma (65%), germ cell tumor (99%) and other solid embryonic tumors [62], implicating its favorable role(s) in childhood cancer forma-

tion. To ascertain the expression of mutant GPC3 in the primary and metastatic osteosarcomas, transcriptome-based Sanger sequencing was conducted, which showed that mutant GPC3 gene was transcribed in primary tumor and in higher levels in its metastatic tissue and spheroids. It is thus the first report about GPC3 mutation and expression in osteosarcoma, and its significant up-regulation in metastatic osteosarcoma. These findings indicate that this genetic alteration may be related to the aggressive behavior of osteosarcoma and the prognosis of patients. In view of the oncogenic effect of GPC3 and the promising application of anti-GPC3 therapy in liver cancer and other tumors, it is reasonable to speculate that GPC3 may be a potential therapeutic target for osteosar-

comas, and the targeted anti-GPC3 drugs used in other types of cancers may be also applicable for the osteosarcomas with GPC3 mutation and/or expression.

Patient-derived tumor spheroids (PDSs) are 3D cultures of cancer cells derived from an individual patient. Because PDSs well maintain the basic biological features of their original tumors, they have been widely used in translational oncology research including the PDS-based prediction of chemo-sensitivity for personalized treatment [63–65]. Recently, the spheroids of established OS cell lines and the pulmonary metastasis of an OS case were successfully cultured [43,44], while the PDSs prepared from original osteosarcoma and bone metastasis remain unavailable. In this study, a pair of primary and bone metastatic PDSs was successfully cultured using the tumor samples of the same OS patient, and drug sensitivity assay was performed on them. The results revealed that primary PDSs were sensitive to the first line anti-OS drugs in the order of carboplatin, ifosfamide, doxorubicin/carboplatin combination and cisplatin, while the metastatic PDSs became tolerable to all of those drugs especially to cisplatin. These results suggest that the metastatic spheroids with the increase of GPC3 mutation abundance (87.06%) acquired the ability of multidrug resistance. RT-PCR and immunofluorescent labeling further demonstrate significant upregulation of GPC3 expression in metastatic tumor (2.04 \times) and its spheroids (1.67 \times) in comparison with that of their primary counterparts. For these reasons, we assumed that GPC3 mutation and upregulation may be responsible for the poor drug response and therefore bone metastasis. Given lack of molecular therapeutic target of OS patients, it would be of therapeutic value if the PDSs, especially the m-OS one of this patient are committed to death by anti-GPC3 approach.

Monoclonal antibody therapy against GPC3 has been used in the clinical treatment of HCCs [45,66,67]. In order to explore the possible application of this therapy to GPC3 + osteosarcoma, four concentrations of GPC3 monoclonal antibodies (0.5, 1, 1.5 and 2 μ g/mL) were used to incubate with the spheroids derived from this multidrug-resistant metastatic OS case. The results showed that the GPC3 antibody effectively inhibited the growth of spheroids and induced apoptosis in a dose-related manner. According to the data of clinical treatment of hepatocellular carcinomas, the anti-GPC3 antibody can sensitize HCC cells to conventional anticancer agents including cisplatin [19]. Because the spheroids of this metastatic OS exhibited strongest acquired resistance to cisplatin in comparison with its response to other drugs, they were treated by anti-GPC3 antibody and cisplatin combination. It was found that neither the low dose of anti-GPC3 antibody (1 μ g/mL) nor 4 μ M cisplatin exerted obvious inhibitory effect on the spheroid but their combination caused remarkable cell death (92.93%). These results thus suggest 1) that GPC3 may be an important factor leading to drug resistance and recurrence in this patient and 2) that GPC3-targeted therapy may be applicable to GPC3-positive OS cases by itself or in combination with other anticancer drugs. Unlike the situation in most human malignancies, no usable genetic alteration has been so far available for targeted osteosarcoma therapy [17]. The findings of this study thus indicate that GPC3 mutation and expression may be the potential therapeutic target of osteosarcomas. Investigation of the generality of OS GPC3 mutation and/or expression in a large panel of OS cases and the therapeutic consequence of mutant or wild type GPC3 inhibition will further support this notion.

Taken together, this study demonstrated for the first time GPC3 mutation in a primary osteosarcoma and the increased abundance and upregulation of mutant GPC3 in its metastatic tumor/spheroids with multidrug resistance. Blockage of GPC3 function with anti-GPC3 antibody efficiently led osteosarcoma spheroids to apoptosis and improved the therapeutic efficacy of cisplatin. Because GPC3-targeting therapy has been used to treat hepatocel-

lular carcinomas and it is also effective to the OS spheroids with multidrug resistance, GPC3-targeting therapy would be a novel approach for better management of osteosarcomas. To further support this notion, we will profile the frequency and expression patterns of GPC3 in sufficient cases of osteosarcomas.

CRediT authorship contribution statement

Jun-Hua Nie: Data curation, Formal analysis, Investigation, Visualization, Writing - original draft, Writing - review & editing. **Tao Yang:** Data curation, Methodology, Validation. **Hong Li:** Conceptualization, Formal analysis, Writing - original draft, Writing - review & editing. **Hai-Shan Ye:** Data curation, Methodology, Validation. **Guo-Qing Zhong:** Data curation, Resources, Validation, Investigation. **Ting-Ting Li:** Data curation, Methodology. **Chi Zhang:** Resources, Validation. **Wen-Han Huang:** Investigation, Resources, Validation. **Jin Xiao:** Resources, Validation. **Zhi Li:** Investigation, Resources. **Jian-Li He:** Software, Data curation, Visualization. **Bo-Le Du:** Software, Data curation, Visualization. **Yu Zhang:** Funding acquisition, Methodology, Project administration, Writing - review & editing. **Jia Liu:** Funding acquisition, Methodology, Project administration, Writing - original draft, Writing - review & editing.

Declaration of Competing Interest

The authors declare that they have no known competing financial interests or personal relationships that could have appeared to influence the work reported in this paper.

Acknowledgements

The authors express gratitude to the doctors in the Department of Clinical Pathology, Guangdong Provincial Hospital for providing the paraffin sections of osteosarcomas. This work was supported by the grants from National Natural Science Foundation of China (No. 31771038), National Key Research and Development Program of China (2017YFB0702604; 2016YFB0700803), the Joint Fund of Ministry of Education for Equipment Pre-research (No. 6141A02022632) to Dr. Yu Zhang and by the grants from National Natural Science Foundation of China (No. 81272786 and 81450016) and the Special Fund of South China University of Technology from Central Government of China to Dr. Jia Liu.

Author's Contributions

Yu Zhang and Jia Liu designed the project and supervise the experiments, data analyses and manuscript writing; Hong Li directed the experiments and drafted the manuscript; Jun-Hua Nie, Hai-Shan Ye and Ting-Ting Li performed the experiments; Jian-Li He and Bo-Le Du performed the genome sequencing and data analysis; Tao Yang, Guo-Qing Zhong, Chi Zhang, Wen-Han Huang and Jin Xiao assist in surgery, sample supplement and clinical data collection and analysis; Zhi Li provided pathological services. All authors read and approved the final manuscript.

References

- [1] M.S. Isakoff, S.S. Bielack, P. Meltzer, R. Gorlick, Osteosarcoma: current treatment and a collaborative pathway to success, *J. Clin. Oncol.* 33 (27) (2015) 3029–3035.
- [2] R.L. Siegel, K.D. Miller, A. Jemal, *Cancer statistics, 2020*, *CA Cancer J. Clin.* 70 (1) (2020) 7–30.
- [3] P.J. Messersmith, R.M. Garcia, F.W. Abdul-Karim, E.M. Greenfield, P.J. Getty, Osteosarcoma, *J. Am. Acad. Orthop. Surg.* 17 (8) (2009) 515–527.
- [4] S. Yoshida, J. Cellaire, C. Pace, C. Taylor, Y. Kaneuchi, S. Evans, A. Abudu, Delay in diagnosis of primary osteosarcoma of bone in children: Have we improved in

- the last 15 years and what is the impact of delay on diagnosis?, *J Bone Oncol* 28 (2021) 100359
- [5] J.S. Whelan, L.E. Davis, Osteosarcoma, chondrosarcoma, and chordoma, *J. Clin. Oncol.* 36 (2) (2018) 188–193.
 - [6] C. Chiappetta, M. Mancini, F. Lessi, P. Aretini, V. De Gregorio, C. Puggioni, R. Carletti, V. Petrozza, P. Civita, S. Franceschi, A.G. Naccarato, C.D. Rocca, C.M. Mazzanti, C. Di Cristofano, Whole-exome analysis in osteosarcoma to identify a personalized therapy, *Oncotarget* 8 (46) (2017) 80416–80428.
 - [7] N. Jaffe, A. Puri, H. Gelderblom, Osteosarcoma: evolution of treatment paradigms, *Sarcoma* 2013 (2013) 203531.
 - [8] L. Mirabello, R.J. Troisi, S.A. Savage, International osteosarcoma incidence patterns in children and adolescents, middle ages and elderly persons, *Int. J. Cancer* 125 (1) (2009) 229–234.
 - [9] L. Kager, A. Zoubek, U. Potechger, U. Kastner, S. Flege, B. Kempf-Bielack, D. Branschkeid, R. Kotz, M. Salzer-Kuntschik, W. Winkelmann, G. Jundt, H. Kabisch, P. Reichardt, H. Jurgens, H. Gagner, S.S. Bielack, G., Cooperative German-Austrian-Swiss Osteosarcoma Study, Primary metastatic osteosarcoma: presentation and outcome of patients treated on neoadjuvant Cooperative Osteosarcoma Study Group protocols, *J. Clin. Oncol.* 21 (10) (2003) 2011–2018.
 - [10] G. Casey, D. Conti, R. Haile, D. Duggan, Next generation sequencing and a new era of medicine, *Gut* 62 (6) (2013) 920–932.
 - [11] I. Martincorena, K.M. Raine, M. Gerstung, K.J. Dawson, K. Haase, P. Van Loo, H. Davies, M.R. Stratton, P.J. Campbell, Universal patterns of selection in cancer and somatic tissues, *Cell* 171(5) (2017) 1029–1041 e21.
 - [12] P.A. Jones, J.P. Issa, S. Baylin, Targeting the cancer epigenome for therapy, *Nat. Rev. Genet.* 17 (10) (2016) 630–641.
 - [13] G. Siravegna, M. Mussolin, M. Buscarino, G. Corti, A. Cassingena, G. Crisafulli, A. Ponzetti, C. Cremolini, A. Amatu, C. Lauricella, S. Lamba, S. Hobor, A. Avallone, E. Valtona, G. Rospo, E. Medico, V. Motta, C. Antoniotti, F. Tatangelo, B. Bellosillo, S. Veronese, A. Budillon, C. Montagut, P. Racca, S. Marsoni, A. Falcone, R.B. Corcoran, F. Di Nicolantonio, F. Loupakis, S. Siena, A. Sartore-Bianchi, A. Bardelli, Clonal evolution and resistance to EGFR blockade in the blood of colorectal cancer patients, *Nat. Med.* 21 (7) (2015) 827.
 - [14] C. Swanton, J.C. Soria, A. Bardelli, A. Biankin, C. Caldas, S. Chandraratnam, L. de Koning, C. Dive, J. Feunteun, S.Y. Leung, R. Marais, E.R. Mardis, N. McGranahan, G. Middleton, S.A. Quezada, J. Rodon, N. Rosenfeld, C. Sotiriou, F. Andre, Consensus on precision medicine for metastatic cancers: a report from the MAP conference, *Ann. Oncol.* 27 (8) (2016) 1443–1448.
 - [15] N., Cancer Genome Atlas, Comprehensive molecular portraits of human breast tumours, *Nature* 490 (7418) (2012) 61–70.
 - [16] A.B. Mariotto, R. Etzioni, M. Hurlbert, L. Penberthy, M. Mayer, Estimation of the number of women living with metastatic breast cancer in the United States, *Cancer Epidemiol Biomarkers Prev* 26 (6) (2017) 809–815.
 - [17] L.C. Slayles, M.R. Breese, A.L. Koehne, S.G. Leung, A.G. Lee, H.Y. Liu, A. Spillinger, A.T. Shah, B. Tanasa, K. Straessler, F.K. Hazard, S.L. Spunt, N. Marina, G.E. Kim, S. J. Cho, R.S. Avedian, D.G. Mohler, M.O. Kim, S.G. DuBois, D.S. Hawkins, E.A. Sweet-Cordero, Genome-informed targeted therapy for osteosarcoma, *Cancer Discov* 9 (1) (2019) 46–63.
 - [18] W.S. El-Deiry, R.M. Goldberg, H.J. Lenz, A.F. Shields, G.T. Gibney, A.R. Tan, J. Brown, B. Eisenberg, E.I. Heath, S. Phuphanich, E. Kim, A.J. Brenner, J.L. Marshall, The current state of molecular testing in the treatment of patients with solid tumors, 2019, *CA Cancer J. Clin.* 69 (4) (2019) 305–343.
 - [19] M. Kansara, M.W. Teng, M.J. Smyth, D.M. Thomas, Translational biology of osteosarcoma, *Nat. Rev. Cancer* 14 (11) (2014) 722–735.
 - [20] H. Aboulkheyr Es, L. Montazeri, A.R. Aref, M. Vosough, H. Baharvand, Personalized cancer medicine: an organoid approach, *Trends Biotechnol.* 36 (4) (2018) 358–371.
 - [21] S. Chen, Y. Zhou, Y. Chen, J. Gu, fastp: an ultra-fast all-in-one FASTQ preprocessor, *Bioinformatics* 34 (17) (2018) i884–i890.
 - [22] H. Li, R. Durbin, Fast and accurate short read alignment with Burrows-Wheeler transform, *Bioinformatics* 25 (14) (2009) 1754–1760.
 - [23] A. McKenna, M. Hanna, E. Banks, A. Sivachenko, K. Cibulskis, A. Kernysky, K. Garimella, D. Altshuler, S. Gabriel, M. Daly, M.A. DePristo, The genome analysis toolkit: a mapreduce framework for analyzing next-generation DNA sequencing data, *Genome Res.* 20 (9) (2010) 1297–1303.
 - [24] K. Cibulskis, M.S. Lawrence, S.L. Carter, A. Sivachenko, D. Jaffe, C. Sougnez, S. Gabriel, M. Meyerson, E.S. Lander, G. Getz, Sensitive detection of somatic point mutations in impure and heterogeneous cancer samples, *Nat. Biotechnol.* 31 (3) (2013) 213–219.
 - [25] E. Talevich, A.H. Shain, T. Botton, B.C. Bastian, CNVkit: genome-wide copy number detection and visualization from targeted DNA sequencing, *PLoS Comput. Biol.* 12 (4) (2016) e1004873.
 - [26] J. Liang, Y. She, J. Zhu, L. Wei, L. Zhang, L. Gao, Y. Wang, J. Xing, Y. Guo, X. Meng, P. Li, Development and validation of an ultra-high sensitive next-generation sequencing assay for molecular diagnosis of clinical oncology, *Int. J. Oncol.* 49 (5) (2016) 2088–2104.
 - [27] K. Wang, M. Li, H. Hakonarson, ANNOVAR: functional annotation of genetic variants from high-throughput sequencing data, *Nucleic Acids Res.* 38 (16) (2010) e164.
 - [28] J. Drost, W.R. Karthaus, D. Gao, E. Driehuis, C.L. Sawyers, Y. Chen, H. Clevers, Organoid culture systems for prostate epithelial and cancer tissue, *Nat. Protoc.* 11 (2) (2016) 347–358.
 - [29] N. Sachs, J. de Ligti, O. Kopper, E. Gogola, G. Bounova, F. Weeber, A.V. Balgobind, K. Wind, A. Gracanin, H. Begthel, J. Korving, R. van Boxtel, A.A. Duarte, D. Lelieveld, A. van Hoeck, R.F. Ernst, F. Blokzijl, I.J. Nijman, M. Hoogstraat, M. van de Ven, D.A. Egan, V. Zinzalla, J. Moll, S.F. Boj, E.E. Voest, L. Wessels, P.J. van Diest, S. Rottenberg, R.G.J. Vries, E. Cuppen, H. Clevers, A living biobank of breast cancer organoids captures disease heterogeneity, *Cell* 172(1–2) (2018) 373–386 e10.
 - [30] X. Xiao, W. Wang, Y. Li, D. Yang, X. Li, C. Shen, Y. Liu, X. Ke, S. Guo, Z. Guo, HSP90AA1-mediated autophagy promotes drug resistance in osteosarcoma, *J. Exp. Clin. Cancer Res.* 37 (1) (2018) 201.
 - [31] M. Fanelli, E. Tavanti, M.P. Patrizio, S. Vella, A. Fernandez-Ramos, F. Magagnoli, S. Luppi, C.M. Hattinger, M. Serra, Cisplatin resistance in osteosarcoma: in vitro validation of candidate DNA repair-related therapeutic targets and drugs for tailored treatments, *Front. Oncol.* 10 (2020) 331.
 - [32] A. Gougelet, D. Pissaloux, A. Besse, J. Perez, A. Duc, A. Dutour, J.Y. Blay, L. Alberti, Micro-RNA profiles in osteosarcoma as a predictive tool for ifosfamide response, *Int. J. Cancer* 129 (3) (2011) 680–690.
 - [33] K. Marley, S.C. Helfand, J. Simpson, J.E. Mata, W.G. Tracewell, L. Brownlee, S. Bracha, B. Seguin, Pharmacokinetic study and evaluation of the safety of taurolidine for dogs with osteosarcoma, *J. Exp. Clin. Cancer Res.* 32 (2013) 74.
 - [34] Y. Zhou, J.K. Shen, Z. Yu, F.J. Hornicek, Q. Kan, Z. Duan, Expression and therapeutic implications of cyclin-dependent kinase 4 (CDK4) in osteosarcoma, *Biochim. Biophys. Acta Mol. Basis Dis.* 1864(5 Pt A) (2018) 1573–1582.
 - [35] T.M. Yang, S.N. Qi, N. Zhao, Y.J. Yang, H.Q. Yuan, B. Zhang, S. Jin, Induction of apoptosis through caspase-independent or caspase-9-dependent pathway in mouse and human osteosarcoma cells by a new nitroxyl spin-labeled derivative of podophyllotoxin, *Apoptosis* 18 (6) (2013) 727–738.
 - [36] M. Fanelli, C.M. Hattinger, S. Vella, E. Tavanti, F. Michelacci, B. Gudeman, D. Barnett, P. Picci, M. Serra, Targeting ABCB1 and ABCB1 with their Specific Inhibitor CBT-1(R) can Overcome Drug Resistance in Osteosarcoma, *Curr. Cancer Drug Targets* 16 (3) (2016) 261–274.
 - [37] L. Grassi, R. Alfonsi, F. Francescangeli, M. Signore, M.L. De Angelis, A. Addario, M. Costantini, E. Flex, A. Cioffi, S. Pizzi, A. Bruselles, M. Pallocca, G. Simone, M. Haoui, M. Falchi, M. Milella, S. Sentinelli, P. Di Matteo, E. Stellacci, M. Gallucci, G. Muto, M. Tartaglia, R. De Maria, D. Bonci, Organoids as a new model for improving regenerative medicine and cancer personalized therapy in renal diseases, *Cell Death Dis.* 10 (3) (2019) 201.
 - [38] L.X. Zhong, Y. Zhang, M.L. Wu, Y.N. Liu, P. Zhang, X.Y. Chen, Q.Y. Kong, J. Liu, H. Li, Resveratrol and STAT inhibitor enhance autophagy in ovarian cancer cells, *Cell Death Discov.* 2 (2016) 15071.
 - [39] D. Fernandez, M. Guerenio, M.A. Lago Huvelle, M. Cercato, M.G. Peters, Signaling network involved in the GPC3-induced inhibition of breast cancer progression: role of canonical Wnt pathway, *J. Cancer Res. Clin. Oncol.* 144 (12) (2018) 2399–2418.
 - [40] W.W. Ren, D.D. Li, X. Chen, X.L. Li, Y.P. He, L.H. Guo, L.N. Liu, L.P. Sun, X.P. Zhang, MicroRNA-125b reverses oxaliplatin resistance in hepatocellular carcinoma by negatively regulating EVA1A mediated autophagy, *Cell Death Dis.* 9 (5) (2018) 547.
 - [41] D. Wang, X. Niu, Z. Wang, C.L. Song, Z. Huang, K.N. Chen, J. Duan, H. Bai, J. Xu, J. Zhao, Y. Wang, M. Zhuo, X.S. Xie, X. Kang, Y. Tian, L. Cai, J.F. Han, T. An, Y. Sun, S. Gao, J. Zhao, J. Ying, L. Wang, J. He, J. Wang, Multiregion sequencing reveals the genetic heterogeneity and evolutionary history of osteosarcoma and matched pulmonary metastases, *Cancer Res.* 79 (1) (2019) 7–20.
 - [42] A. Hosseini, A. Mirzaei, V. Salimi, K. Jamshidi, P. Babaheidarian, S. Fallah, Z. Rampisheh, N. Khademian, Z. Abdolvahabi, M. Bahrabadi, M. Ibrahim, F. Hosami, M. Tavakoli-Yaraki, The local and circulating SOX9 as a potential biomarker for the diagnosis of primary bone cancer, *J. Bone Oncol.* 23 (2020) 100300.
 - [43] J. Munoz-Garcia, C. Jubeli, A. Loussouarn, M. Goumard, L. Griscmond, A. Renodon-Corniere, M. Heymann, D. Heymann, In vitro three-dimensional cell cultures for bone sarcomas, *J. Bone Oncol.* 30 (2021) 100379.
 - [44] A. He, Y. Huang, W. Cheng, D. Zhang, W. He, Y. Bai, C. Gu, Z. Ma, Z. He, G. Si, B. Chen, D.T. Breault, M. Dong, D. Xiang, Organoid culture system for patient-derived lung metastatic osteosarcoma, *Med. Oncol.* 37 (11) (2020) 105.
 - [45] Y. Shimizu, T. Suzuki, T. Yoshikawa, I. Endo, T. Nakatsura, Next-generation cancer immunotherapy targeting glypican-3, *Front. Oncol.* 9 (2019) 248.
 - [46] L. Mirabello, R.J. Troisi, S.A. Savage, Osteosarcoma incidence and survival rates from 1973 to 2004: data from the surveillance, epidemiology, and end results program, *Cancer* 115 (7) (2009) 1531–1543.
 - [47] Y. Yang, L. Han, Z. He, X. Li, S. Yang, J. Yang, Y. Zhang, D. Li, Y. Yang, Z. Yang, Advances in limb salvage treatment of osteosarcoma, *J. Bone Oncol.* 10 (2018) 36–40.
 - [48] N.M. Bernthal, N. Federman, F.R. Eilber, S.D. Nelson, J.J. Eckardt, F.C. Eilber, W. D. Tap, Long-term results (>25 years) of a randomized, prospective clinical trial evaluating chemotherapy in patients with high-grade, operable osteosarcoma, *Cancer* 118 (23) (2012) 5888–5893.
 - [49] M.P. Link, A.M. Goorin, A.W. Miser, A.A. Green, C.B. Pratt, J.B. Belasco, J. Pritchard, J.S. Malpas, A.R. Baker, J.A. Kirkpatrick, et al., The effect of adjuvant chemotherapy on relapse-free survival in patients with osteosarcoma of the extremity, *N. Engl. J. Med.* 314 (25) (1986) 1600–1606.
 - [50] S. Salah, R. Ahmad, I. Sultan, S. Yaser, A. Shehadeh, Osteosarcoma with metastasis at initial diagnosis: current outcomes and prognostic factors in the context of a comprehensive cancer center, *Mol. Clin. Oncol.* 2 (5) (2014) 811–816.
 - [51] M.F. Berger, E.R. Mardis, The emerging clinical relevance of genomics in cancer medicine, *Nat. Rev. Clin. Oncol.* 15 (6) (2018) 353–365.
 - [52] Y. Chen, T. Wang, M. Huang, Q. Liu, C. Hu, B. Wang, D. Han, C. Chen, J. Zhang, Z. Li, C. Liu, W. Lei, Y. Chang, M. Wu, D. Xiang, Y. Chen, R. Wang, W. Huang, Z. Lei, X. Chu, MAFB promotes cancer stemness and tumorigenesis in osteosarcoma

- through a Sox9-mediated positive feedback loop, *Cancer Res.* 80 (12) (2020) 2472–2483.
- [53] L.A. Duhamel, H. Ye, D. Halai, B.D. Idowu, N. Presneau, R. Tirabosco, A.M. Flanagan, Frequency of mouse double minute 2 (MDM2) and mouse double minute 4 (MDM4) amplification in parosteal and conventional osteosarcoma subtypes, *Histopathol* 60 (2) (2012) 357–359.
- [54] K.H. Lu, S.C. Su, C.W. Lin, Y.H. Hsieh, Y.C. Lin, M.H. Chien, R.J. Reiter, S.F. Yang, Melatonin attenuates osteosarcoma cell invasion by suppression of C-C motif chemokine ligand 24 through inhibition of the c-Jun N-terminal kinase pathway, *J. Pineal Res.* 65 (3) (2018) e12507.
- [55] X. He, Z. Pang, X. Zhang, T. Lan, H. Chen, M. Chen, H. Yang, J. Huang, Y. Chen, Z. Zhang, W. Jing, R. Peng, H. Zhang, Consistent amplification of FRS2 and MDM2 in low-grade osteosarcoma: a genetic study of 22 cases with clinicopathologic analysis, *Am. J. Surg. Pathol.* 42 (9) (2018) 1143–1155.
- [56] Y. Suehara, D. Alex, A. Bowman, S. Middha, A. Zehir, D. Chakravarty, L. Wang, G. Jour, K. Nafa, T. Hayashi, A.A. Jungbluth, D. Frosina, E. Slotkin, N. Shukla, P. Meyers, J.H. Healey, M. Hameed, M. Ladanyi, Clinical genomic sequencing of pediatric and adult osteosarcoma reveals distinct molecular subsets with potentially targetable alterations, *Clin. Cancer Res.* 25 (21) (2019) 6346–6356.
- [57] J. Yang, M. Annala, P. Ji, G. Wang, H. Zheng, D. Codgell, X. Du, Z. Fang, B. Sun, M. Nykter, K. Chen, W. Zhang, Recurrent LRP1-SNRNP25 and KCNMB4-CCND3 fusion genes promote tumor cell motility in human osteosarcoma, *J. Hematol. Oncol.* 7 (2014) 76.
- [58] S. Gupta, T. Ito, D. Alex, C.M. Vanderbilt, J.C. Chang, N. Islamdoust, Y. Zhang, K. Nafa, J. Healey, M. Ladanyi, M.R. Hameed, RUNX2 (6p21.1) amplification in osteosarcoma, *Hum. Pathol.* 94 (2019) 23–28.
- [59] Z. Zhao, Q. Jia, M.S. Wu, X. Xie, Y. Wang, G. Song, C.Y. Zou, Q. Tang, J. Lu, G. Huang, J. Wang, D.C. Lin, H.P. Koeffler, J.Q. Yin, J. Shen, Degalactotigonin, a natural compound from solanum nigrum L., inhibits growth and metastasis of osteosarcoma through GSK3beta inactivation-mediated repression of the Hedgehog/Gli1 pathway, *Clin. Cancer Res.* 24 (1) (2018) 130–144.
- [60] M. Capurro, I.R. Wanless, M. Sherman, G. Deboer, W. Shi, E. Miyoshi, J. Filmus, Glypican-3: a novel serum and histochemical marker for hepatocellular carcinoma, *Gastroenterology* 125 (1) (2003) 89–97.
- [61] F. Zhou, W. Shang, X. Yu, J. Tian, Glypican-3: A promising biomarker for hepatocellular carcinoma diagnosis and treatment, *Med. Res. Rev.* 38 (2) (2018) 741–767.
- [62] M.V. Ortiz, S.S. Roberts, J. Glade Bender, N. Shukla, L.H. Wexler, Immunotherapeutic targeting of GPC3 in pediatric solid embryonal tumors, *Front. Oncol* 9 (2019) 108.
- [63] H. Tiriaci, P. Belleau, D.D. Engle, D. Plenker, A. Deschenes, T.D.D. Somerville, F.E. M. Froeling, R.A. Burkhart, R.E. Denroche, G.H. Jang, K. Miyabayashi, C.M. Young, H. Patel, M. Ma, J.F. LaComb, R.L.D. Palmira, A.A. Javed, J.C. Huynh, M. Johnson, K. Arora, N. Robine, M. Shah, R. Sanghvi, A.B. Goetz, C.Y. Lowder, L. Martello, E. Driehuis, N. LeComte, G. Askan, C.A. Iacobuzio-Donahue, H. Clevers, L.D. Wood, R.H. Hruban, E. Thompson, A.J. Aguirre, B.M. Wolpin, A. Sasson, J. Kim, M. Wu, J.C. Bucobo, P. Allen, D.V. Sejjal, W. Nealon, J.D. Sullivan, J.M. Winter, P.A. Gimotty, J.L. Grem, D.J. DiMaio, J.M. Buscaglia, P.M. Grandgenett, J.R. Brody, M.A. Hollingsworth, G.M. O’Kane, F. Notta, E. Kim, J. M. Crawford, C. Devoe, A. Ocean, C.L. Wolfgang, K.H. Yu, E. Li, C.R. Vakoc, B. Hubert, S.E. Fischer, J.M. Wilson, R. Moffitt, J. Knox, A. Krasnitz, S. Gallinger, D. A. Tuveson, Organoid profiling identifies common responders to chemotherapy in pancreatic cancer, *Cancer Discov.* 8 (9) (2018) 1112–1129.
- [64] K. Ganesh, C. Wu, K.P. O’Rourke, B.C. Szeglin, Y. Zheng, C.G. Sauve, M. Adileh, I. Wasserman, M.R. Marco, A.S. Kim, M. Shady, F. Sanchez-Vega, W.R. Karthaus, H.H. Won, S.H. Choi, R. Pelosof, A. Barlas, P. Ntiamoah, E. Pappou, A. Elghouayel, J.S. Strong, C.T. Chen, J.W. Harris, M.R. Weiser, G.M. Nash, J.G. Guillem, I.H. Wei, R.N. Kolesnick, H. Veeraraghavan, E.J. Ortiz, I. Petkovska, A. Cercek, K.O. Manova-Todorova, L.B. Saltz, J.A. Lavery, R.P. DeMatteo, J. Massague, P.B. Paty, R. Yaeger, X. Chen, S. Patil, H. Clevers, M.F. Berger, S.W. Lowe, J. Shia, P.B. Romesser, L.E. Dow, J. Garcia-Aguilar, C.L. Sawyers, J.J. Smith, A rectal cancer organoid platform to study individual responses to chemoradiation, *Nat. Med.* 25 (10) (2019) 1607–1614.
- [65] O. Kopper, C.J. de Witte, K. Lohmussaar, J.E. Valle-Inclan, N. Hami, L. Kester, A. V. Balgobind, J. Korving, N. Proost, H. Begthel, L.M. van Wijk, S.A. Revilla, R. Theeuwssen, M. van de Ven, M.J. van Roosmalen, B. Ponsioen, V.W.H. Ho, B.G. Neel, T. Bosse, K.N. Gaarenstroom, H. Vrieling, M.P.G. Vreeswijk, P.J. van Diest, P.O. Witteveen, T. Jonges, J.L. Bos, A. van Oudenaarden, R.P. Zweemer, H.J.G. Snippet, W.P. Kloosterman, H. Clevers, An organoid platform for ovarian cancer captures intra- and interpatient heterogeneity, *Nat. Med.* 25 (5) (2019) 838–849.
- [66] G.K. Abou-Alfa, O. Puig, B. Daniele, M. Kudo, P. Merle, J.W. Park, P. Ross, J.M. Peron, O. Ebert, S. Chan, T.P. Poon, M. Colombo, T. Okusaka, B.Y. Ryoo, B. Minguez, T. Tanaka, T. Ohtomo, S. Ukrainskyj, F. Boisserie, O. Rutman, Y.C. Chen, C. Xu, E. Shochat, L. Jukofsky, B. Reis, G. Chen, L. Di Laurenzio, R. Lee, C.J. Yen, Randomized phase II placebo controlled study of codrituzumab in previously treated patients with advanced hepatocellular carcinoma, *J. Hepatol.* 65 (2) (2016) 289–295.
- [67] J. Fu, H. Wang, Precision diagnosis and treatment of liver cancer in China, *Cancer Lett.* 412 (2018) 283–288.